Indication of subdominant d-wave interaction in superconducting CaKFe_{4}As_{4}

D. Jost, J.-R. Scholz, U. Zweck, W. R. Meier, A. E. Böhmer, P. C. Canfield, N. Lazarević, and R. Hackl

Phys. Rev. B **98**, 020504 — Published 13 July 2018

DOI: 10.1103/PhysRevB.98.020504

Subdominant d-wave interaction in superconducting $CaKFe_4As_4$?

D. Jost,[1,2] J.-R. Scholz,[1,2] U. Zweck,[1,2] W. R. Meier,[3,4]
A. E. Böhmer,[4,*] P. C. Canfield,[4,3] N. Lazarević,[5] and R. Hackl[1]

[1] *Walther Meissner Institut, Bayerische Akademie der Wissenschaften, 85748 Garching, Germany*
[2] *Fakultät für Physik E23, Technische Universität München, 85748 Garching, Germany*
[3] *Department of Physics and Astronomy, Iowa State University, Ames, Iowa 50011, USA*
[4] *Division of Materials Science and Engineering, Ames Laboratory, Ames, Iowa 50011, USA*
[5] *Center for Solid State Physics and New Materials, Institute of Physics Belgrade, University of Belgrade, Pregrevica 118, 11080 Belgrade, Serbia*

(Dated: June 26, 2018)

We report inelastic light scattering results on the stoichiometric and fully ordered superconductor $CaKFe_4As_4$ as a function of temperature and light polarization. In the energy range between 10 and 315 cm^{-1} (1.24 and 39.1 meV) we observe the particle-hole continuum above and below the superconducting transition temperature T_c and 7 of the 8 Raman active phonons. The main focus is placed on the analysis of the electronic excitations. Below T_c all three symmetries projected with in-plane polarizations display a redistribution of spectral weight characteristic for superconductivity. The energies of the pair-breaking peaks in A_{1g} and B_{2g} symmetry are in approximate agreement with the results from photoemission studies. In B_{1g} symmetry the difference between normal and superconducting state is most pronounced, and the feature is shifted downwards with respect to those in A_{1g} and B_{2g} symmetry. The maximum peaking at 134 cm^{-1} (16.6 meV) has a substructure on the high-energy side. We interpret the peak at 134 cm^{-1} in terms of a collective Bardasis-Schrieffer (BS) mode and the substructure as a remainder of the pair-breaking feature on the electron bands. There is a very weak peak at 50 cm^{-1} (6.2 meV) which is tentatively assigned to another BS mode.

PACS numbers: 74.70.Xa, 74.20.Mn, 74.25.nd

$CaKFe_4As_4$ is among the few iron-based compounds which are superconducting at high transition temperature T_c at stoichiometry[1] since the Ca and K atoms form alternating intact layers as shown in Fig. 1. The high degree of order allows one to get as close to the intrinsic properties of the material class as possible since the effects of disorder are expected to be negligible or at least significantly smaller than in solid solutions such as $Ba_{1-x}K_xFe_2As_2$ or $Ba(Fe_{1-x}Co_x)_2As_2$. For instance the residual resistivity ratio (RRR) reaches 15 and is much higher than for $Ba(Fe_{1-x}Co_x)_2As_2$ and comparable or better than for $Ba_{1-x}K_xFe_2As_2$ [2]. Other transport and the thermodynamic properties[2] highlight the similarities to optimally or overdoped $Ba_{1-x}K_xFe_2As_2$.

These similarities include the electronic structure, in particular the Fermi surfaces [Fig. 1 (c)] and the superconducting energy gaps[3]. The gaps were found to be rather isotropic on the individual bands having values of $2\Delta_\alpha = 21$ meV, $2\Delta_\beta = 24$ meV, $2\Delta_\gamma = 16$ meV and $2\Delta_\delta = 24$ meV on the three hole bands (α, β, γ) and the electron band (δ), respectively. The good nesting observed between the β and δ bands was considered to support s-wave interband pairing[3–5] as proposed earlier for the iron-based materials in general[6].

Since there is also nesting among the electron bands one can expect a competing pairing interaction with d-wave symmetry as a subleading instability[7]. Indications thereof were found recently in Raman scattering experiments on $Ba_{1-x}K_xFe_2As_2$.[8–10] The subleading channel manifests itself as a narrow line below the gap edge given that the gap is clean as, e.g., in $Ba_{1-x}K_xFe_2As_2$.[11–13]

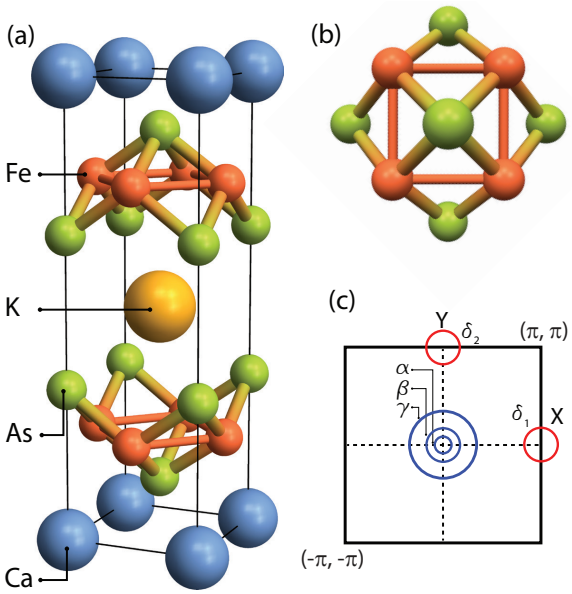

Figure 1. Structure and Fermi surface of $CaKFe_4As_4$. (a) Tetragonal unit cell with the Ca, K, Fe, and As atoms shown in blue, gold, red, and respectively, green[1]. (b) Quasi 2D Fe_2As_2 layer with the full orange line depicting the 1 Fe unit cell. (c) Brillouin zone of the 1 Fe cell. The three hole bands labeled α, β, and γ (blue) encircle the Γ point. The electron bands δ_1 and δ_2 (red) are centered at the X and Y point, respectively [adopted from Mou *et al.*[3]].

The bound state has its origin in a phase fluctuation of the condensate of Cooper pairs. The experimental iden-

tification of this excitation as a Bardasis-Schrieffer (BS) exciton rests on the shape of the line, its temperature dependence and the spectral weight transfer from the pair-breaking feature to the in-gap mode as described in detail in Refs. 9 and 10.

Given its nearly clean gap and the high crystal quality, $CaKFe_4As_4$ is an excellent candidate for scrutinizing the superconducting properties of hole doped 122 systems. We aim at answering the question as to whether or not subleading channels can also be observed in systems other than $Ba_{1-x}K_xFe_2As_2$ and can be identified as generic.

Calibrated Raman scattering equipment was used for the experiments. The sample was attached to the cold finger of a He-flow cryostat. For excitation a diode-pumped solid state laser emitting at 575 nm (Coherent GENESIS MX-SLM 577-500) was used. The polarization of the incoming light was adjusted in a way that the light inside the sample had the proper polarization state. The absorbed power (inside the sample) was set at typically $P_a = 2\,\mathrm{mW}$ independent of polarization. By setting the polarizations of the incident and scattered photons the four symmetries A_{1g}, A_{2g}, B_{1g}, and B_{2g} of the D_{4h} space group can be accessed. For the symmetry assignment we use the 1 Fe unit cell [see Fig. 1 (b) and (c)] since the density of states at the Fermi energy E_F is nearly entirely derived from Fe orbitals. The related projections in the first Brillouin zone (BZ) are visualized in Fig. S1 of the Supplemental Material[14]. In this work the focus is placed on low energies, where A_{2g} is negligibly small. The polarization combinations RR, xy, and $x'y'$ almost exclusively project the A_{1g}, B_{2g}, and B_{1g} symmetries as desired. Here x and y are horizontal and vertical, respectively, in the laboratory system. Note that the out-of-phase vibration of the Fe atoms appears in B_{2g} symmetry in the 1 Fe unit cell rather than in B_{1g} symmetry of the crystallographic unit cell hosting two Fe atoms per Fe_2As_2 plane[14]. The spectra are represented as response functions $R\chi''(T),\Omega)$ which are obtained by dividing the measured cross section by the thermal Bose factor $\{1+n(\Omega,T)\} = \{1+[\exp(\hbar\omega/k_BT)-1]^{-1}\}$. R is an experimental constant.

The $CaKFe_4As_4$ single crystals were grown from the FeAs flux and characterized thoroughly as described by Meier and coworkers[2,15]. The T_c value of $35.21 \pm 0.10\,\mathrm{K}$ we found here is in the range $35.0 \pm 0.2\,\mathrm{K}$ determined by Meier *et al.* (see Fig. S3 in the Supplemental Material[14]). The crystal structure of $CaKFe_4As_4$ is very similar to that of AFe_2As_2 systems [cf. Fig. 1 (a)] and belongs to the tetragonal D_{4h} space group. Since $CaKFe_4As_4$ has alternating Ca and K planes between the Fe_2As_2 layers the point group is simple-tetragonal ($P4/mmm$)[1] rather than the body-centered tetragonal ($I4/mmm$) as $BaFe_2As_2$ [16].

Figure 2 shows the normal (red) and superconducting (blue) Raman spectra of $CaKFe_4As_4$ at the three polarization configurations (a) RR, (b) xy, and (c) $x'y'$. The sample is rotated by 45° with respect to the orientation in Figs. 1 in order to suppress any c-axis projection in the B_{1g} spectra (xy in the laboratory system). Superimposed on the particle-hole continua we observe six and four phonons in RR and $x'y'$ polarization, respectively[17], which will be discussed in the Supplemental Material[14]. As intended there are no phonons in xy configuration, and the spectrum in the normal state is completely smooth to within the experimental error. The structure-less shape indicates that there is no polarization leakage and, more importantly, that there is no defect-induced scattering from phonons highlighting the high crystal quality.

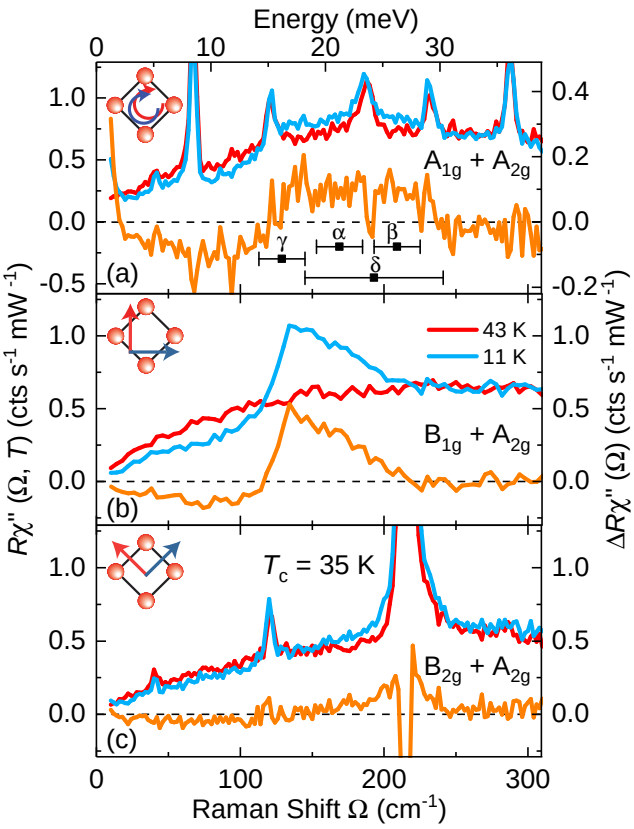

Figure 2. Raman response in $CaKFe_4As_4$ at symmetries and polarizations as indicated. Shown are raw data for $T \ll T_c$ (blue), $T > T_c$ (red) and difference spectra (orange). Phonon modes are present in the A_{1g} and B_{2g} spectra. (a) The pair-breaking maximum extends from $\Omega_0^{(A1g)} = 120 \pm 2\,\mathrm{cm}^{-1}$ to $\Omega_m \approx 230\,\mathrm{cm}^{-1}$. The gap energies $2\Delta_i$ for the four bands i observed by ARPES[3] are reproduced as horizontal bars. Note that the right vertical axis is expanded by a factor of 2.5 with respect to the left one. (b) The B_{1g} pair-breaking peak is well defined and sets on at $\Omega_0^{(B1g)} = 116 \pm 5\,\mathrm{cm}^{-1}$. The dashed line at low energies indicates the expected spectral dependence for a clean gap. (c) The weak B_{2g} pair-breaking peak is located slightly above $2\Delta_\beta$. The intersection of the normal and superconducting spectra is close to $\Omega_0^{(B2g)} = 130 \pm 5\,\mathrm{cm}^{-1}$.

We focus now exclusively on the electronic continua. To this end we also plot the difference spectra,

$$\Delta R\chi''(\Omega) = R\chi''(T = 11\,\mathrm{K}, \Omega) - R\chi''(T = 43\,\mathrm{K}), \quad (1)$$

(orange in Fig. 2) along with the raw data of each polarization configuration. In the difference spectra $\Delta R\chi''(\Omega)$ temperature-independent structures such as (most of) the phonons and the presumably weak and temperature-independent luminescence contributions are eliminated. In this way the changes induced by superconductivity are highlighted.

All spectra show the typical changes upon entering the superconducting state: (i) The opening of the gap induces a suppression of the intensity below a cross-over energy of $\Omega_0 = 125$, 115, and 130 cm^{-1} for A_{1g}, B_{1g}, and B_{2g} symmetry, respectively. In this range $\Delta R\chi''(\Omega)$ (orange) is negative. (ii) The intensity piles up above Ω_0 due to a coherent superposition of pair-breaking and Bogoliubov quasiparticle excitations across the gap 2Δ. The amplitude of the redistribution is small in A_{1g} and B_{2g} symmetry (Fig. 2 (a) and (c) and Figs. S4 and S6 of Ref. [14]) but pronounced in B_{1g} symmetry. [Fig. 2 (b) and Fig. S5 of Ref. [14]]. In the A_{1g} response [Fig. 2 (a)] the signal at $\Omega \to 0$ is enhanced because of surface layers of accumulating residual gas molecules at low temperature (see Fig. S4 of Ref. [14]) and the insufficient suppression of the elastically scattered light in the case of parallel light polarizations (RR here).

The first striking observation is the nearly symmetry-independent cross-over energy Ω_0 where the normal (red) and superconducting (blue) spectra intersect each other or where $\Delta R\chi''(\Omega)$ changes sign. Yet, the intensity for $\Omega < \Omega_0$ does not vanish entirely as expected for a clean gap but is only reduced. No additional structures are observed in the A_{1g} and B_{2g} spectra while a weak hump appears at approximately 50 cm^{-1} [see Fig. 2 (b) and asterisks in Fig. 3 (c) to (e)] in B_{1g} symmetry as can also be seen in in Fig. S5 of Ref. [14].

Second, whereas the normal and the superconducting spectra merge at similar energies close to $\Omega_m = 230\,\mathrm{cm}^{-1}$ in all symmetries the distribution of spectral weight in the range $\Omega_0 < \Omega < \Omega_m$ varies substantially. In none of the symmetries the pair-breaking features display the typical shape. The pair-breaking maximum in B_{2g} symmetry is found at approximately 215 cm^{-1} right underneath the Fe phonon. The negative intensity at 215 cm^{-1} shows that the phonon is renormalized below T_c, and an influence of this renormalization on the electronic features cannot be excluded. However, the gap below 130 cm^{-1} indicates the presence of an intensity redistribution below T_c. In A_{1g} symmetry a wide plateau is observed between Ω_0 and Ω_m. Finally in B_{1g} symmetry, a pronounced peak is found at 135 cm^{-1} above which the intensity decays. Upon studying various temperatures a secondary maximum at about 165 cm^{-1} can be resolved as shown in Fig. S5 of Ref. [14].

For the discussion below we additionally plot in Fig. 2 (a) the gap energies $2\Delta_i$ as horizontal bars according to a recent photoemission study[3], where i is the band index [c.f. Fig. 1 (c)]. The width of the bars corresponds to the error bars of order $\pm 10\%$ indicated there.

We now discuss the possible interpretations of the electronic Raman spectra presented above. Can the spectra be interpreted exclusively in terms of pair-breaking or are collective modes, similarly as in $Ba_{1-x}K_xFe_2As_2$, necessary for a more consistent explanation?

Using yellow excitation we find a strong redistribution of spectral weight in B_{1g} symmetry similarly as in a simultaneous Raman study using red photons[18] (Note that B_{1g} and B_{2g} are interchanged in the two studies.) With yellow photons we observe the redistribution in all three symmetry channels. As already noticed earlier this difference in the experimental results may be traced back to orbital dependent resonance effects[10]. In contrast to Zhang and coworkers[18] we find finite intensity in the range below the maximal gap at approximately 215 cm^{-1} similar as in $Ba_{1-x}K_xFe_2As_2$. We attribute this intensity predominantly to the multi-gap structure in both compounds. Since there is an intensity redistribution below T_c in all channels we do not believe that there is a strong background at low energies from, e.g., luminescence which has an intensity comparable to that of particle-hole excitations.

The highest pair-breaking energy in our study is observed in B_{2g} symmetry implying a maximal gap energy of $2\Delta_{max} \approx 215\,\mathrm{cm}^{-1}$. This energy corresponds to $\Delta_{max} = 13.3$ meV slightly higher than the largest gaps derived for the β and δ bands, $\Delta_{\beta,\delta} = 12$ meV using angle-resolved photoemission spectroscopy (ARPES)[3]. 215 cm^{-1} coincides with the edge of the A_{1g} pair-breaking feature [see Fig. 2], and we conclude that the ARPES data slightly underestimate the gap energies found by Raman scattering as already observed for $Ba_{1-x}K_xFe_2As_2$ [8 and 9]. Similarly, the lowest gap energy of $\Delta_\gamma = 8$ meV is below 9.3 meV expected from the lower edge in the A_{1g} spectra. There are no structures in the A_{1g} and B_{2g} spectra which one could associate with the gap energy on the α band, $\Delta_\alpha = 10.5$ meV, obtained from ARPES. On this basis we conclude that the maximal gap energies derived from the A_{1g} and B_{2g} Raman spectra are in the same range of approximately $9\,k_B T_c$ as in $Ba_{1-x}K_xFe_2As_2$ close to optimal doping[9].

The question arises whether ARPES and Raman results are compatible with the selection rules. As shown in Fig. S1 of Ref. [14] all bands should be visible in A_{1g} symmetry with comparable weight upon neglecting resonance effects. In fact, all energies are represented in the spectra shown in Fig. 2 (a). Even if a Leggett mode contributes to the A_{1g} spectra, as suggested recently[19], this conclusion survives since the Leggett modes are expected close to the maximal gap energies in the Fe-based systems. The B_{2g} spectra are less easily to be reconciled with this scenario since the gaps on the hole bands should be projected with a similar spectral weight as that of the electron band. Yet we find only a contribution from the largest gap. Although the overall intensity is very weak here the absence of contributions from the γ band cannot be explained by the variation of the peak height with $|\Delta|^2$ [20] or by applying the symmetry selection rules. Either a phenomenological treatment as for $Ba_{1-x}K_xFe_2As_2$ [9] or

a detailed resonance study needs to be performed which, however, is beyond the scope of this work.

Given that the single particle gap energies are by and large reproduced in the A_{1g} and B_{2g} spectra it is important to understand the B_{1g} spectra. As shown in Fig. 2 (c) the energies appearing there are well below those of the A_{1g} and B_{2g} spectra. This is particularly surprising as the δ bands are expected to be projected fully (and not marginally) in B_{1g} symmetry (see Fig. S1 of Ref. [14]) as opposed to all hole bands. Thus, the argument that the strongest peak in the B_{1g} spectra results from the γ band can be discarded. Since in contrast to $Ba(Fe_{1-x}Co_x)_2As_2$ [21 and 22], $NaFe_{1-x}Co_xAs$ [23] or FeSe [24 and 25] there is no nematic phase and the related fluctuations in $CaKFe_4As_4$ an interpretation of the observation in B_{1g} symmetry in terms of nematic fluctuations would be far fetched.

As a consequence there remains only one scenario which reconciles the results observed in the three Raman active symmetries and the ARPES results: The B_{1g} spectra do not directly reflect gap energies but rather are shifted downward by final state interaction as discussed for $Ba_{1-x}K_xFe_2As_2$ in earlier work[8–10]. The similarity can be observed directly by comparing the data in Fig. 3. The difference spectra as a function of temperature indicate that the B_{1g} peak has a robust shoulder on the high-energy side. The overall shape is surprisingly similar to the spectra of $Ba_{0.65}K_{0.35}Fe_2As_2$.

Following this reasoning we identify the maximum of the B_{1g} spectra at 134 cm^{-1} with a collective mode pulled off of the maximal gap energy on the δ band due to a $d_{x^2-y^2}$ wave subleading interaction among the two electron bands as predicted theoretically[13] and observed in $Ba_{1-x}K_xFe_2As_2$. The hump at approximately 165 cm^{-1} is then the remaining intensity of the pair-breaking peak on the δ band after switching on the final state interaction which induces a transfer of intensity from the pair-breaking peak into the bound state[9,12,13]. Only in this way the missing intensity in the range of $2\Delta_\delta$ can be explained consistently.

It is tempting, yet a bit speculative, to explain the faint peak close to 50 cm^{-1} ($2\,k_BT_c$) in terms of a second BS mode in a similar fashion as in $Ba_{1-x}K_xFe_2As_2$ [10]. This would mean that the subdominant coupling is already very strong, and $CaKFe_4As_4$ is on the brink of a d-wave instability. The very weak intensity of the peak argues in this direction since the BS mode is expected to vanish when d-wave pairing wins[10]. Yet, the vanishingly small intensity is also the Achilles heel of the argumentation, and we refrain from going beyond pointing out this possibility. A robust statement is possible only on the basis of improved counting statistics and a microscopic model, which includes the derivation of the eigenvectors of the subdominant pairing channels, as proposed for $Ba_{1-x}K_xFe_2As_2$ [10]. Such an expensive theoretical treatment is beyond the scope of this experimental study.

In summary, we investigated the recently discovered superconductor $CaKFe_4As_4$ with inelastic light scatter-

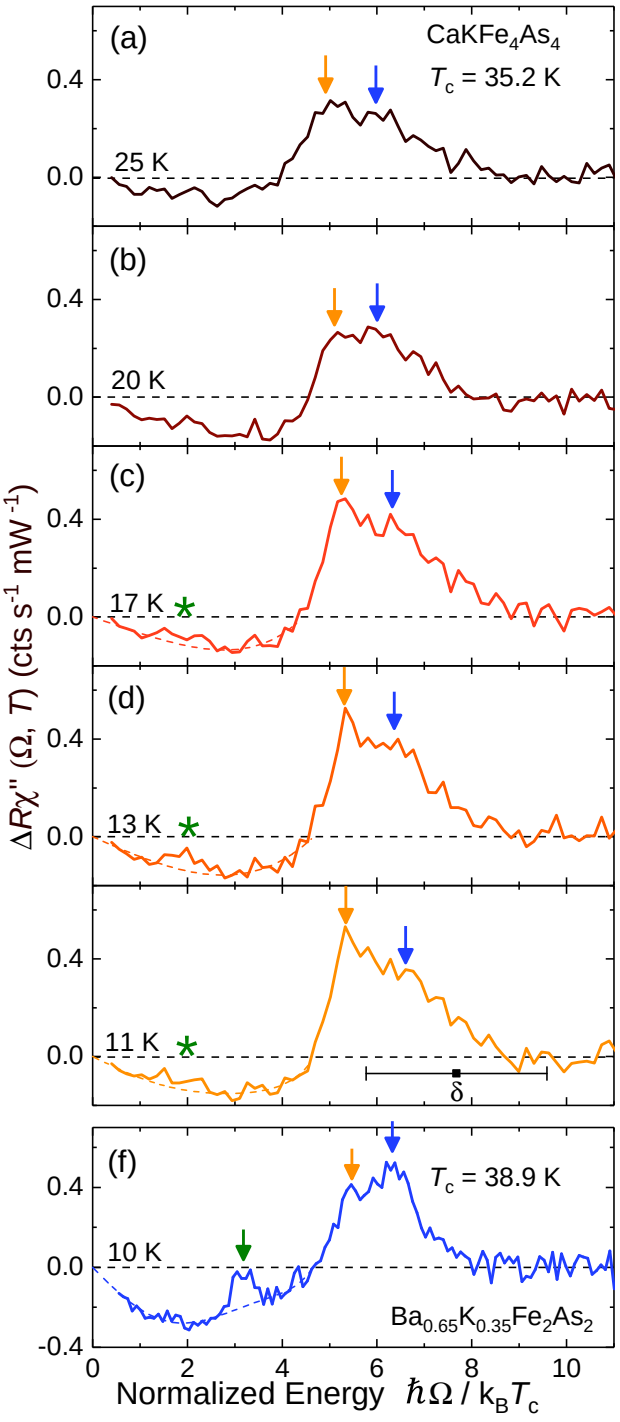

Figure 3. Difference spectra of the B_{1g} Raman response in $CaKFe_4As_4$ and $Ba_{1-x}K_xFe_2As_2$ for temperatures as indicated. For raw data c.f. Fig. 2 and S5 of Ref. [14]. The main peak exhibits a double structure (orange and blue arrows). A second hump is visible in the spectra at 11, 13, and 17 K (asterisks) above the spectral shape expected for a clean gap (colored dashes). (f) Difference spectrum of $Ba_{0.65}K_{0.35}As_2Fe_2$. From[10]. The arrows show two Bardasis-Schrieffer modes at 3.1 (green arrow) and 5.2 k_BT_c (orange arrow). The remainder of the pair breaking peak is located at 6.2 k_BT_c (blue arrow) since the high-energy part is drained into the BS modes.

ing as a function of photon polarisation and temperature. Using yellow light (575 nm) superconducting features were found in A_{1g}, B_{1g} and B_{2g} symmetry.

A weak but well-defined pair-breaking feature is found at 215 cm^{-1} (corresponding to $\Delta = 13.3$ meV) in B_{2g} symmetry which is slightly above the largest gaps observed by ARPES for the β and the δ bands[3] and close to the energy Ω_m where the normal and the superconducting spectra merge in all symmetry projections. This feature is also present in the A_{1g} spectra. In addition to the high-energy feature the A_{1g} intensity displays a plateau-like shape down to $\Omega_0^{(A1g)} = 125\,cm^{-1}$. Given the small discrepancies between the gap energies derived from the ARPES data and the Raman spectra one can conclude that the A_{1g} spectra reflect the entire range of gap energies of $CaKFe_4As_4$ even though the individual gap energies cannot be resolved.

In B_{1g} symmetry, the superconducting feature is centered at lower energy than in the two other symmetries. We interpret the sharp maximum at 134 cm^{-1} as a collective Bardasis-Schrieffer mode pulled off of the maximal gap on the δ band similarly as in the sister compound $Ba_{0.65}K_{0.35}Fe_2As_2$. The shoulder at approximately 165 cm^{-1} is a remainder of the pair-breaking peak losing most of its intensity to the collective mode[9,13]. Whether or not the weak structure at 50 cm^{-1} is another BS mode with even stronger coupling cannot be decided with certainty because of the fading intensity. If this interpretation could be supported further $CaKFe_4As_4$ would be closer to a d-wave instability than $Ba_{1-x}K_xFe_2As_2$. The smaller T_c of $CaKFe_4As_4$ argues in this direction since a strong d pairing channel frustrates the s-wave ground state and reduces T_c. Even without dwelling on the peak at 50 cm^{-1} we may conclude that $CaKFe_4As_4$ is a true sibling of $Ba_{1-x}K_xFe_2As_2$[10] thus demonstrating that pairing fingerprints can be observed preferably in materials with clean gaps.

ACKNOWLEDGEMENTS

We acknowledge valuable discussions with G. Blumberg. The work was supported by the Friedrich-Ebert-Stiftung, the Transregional Collaborative Research Center TRR 80, and the Serbian Ministry of Education, Science and Technological Development under Project III45018. We acknowledge support by the DAAD through the bilateral project between Serbia and Germany (grant numbers 56267076 and 57142964). Work at Ames Laboratory was supported by the U.S. Department of Energy, Office of Basic Energy Sciences, Division of Materials Sciences and Engineering under Contract No. DE-AC02- 07CH11358. W.R.M. was supported by the Gordon and Betty Moore Foundations EPiQS Initiative through Grant No. GBMF4411.

* Present address: Karlsruher Institut für Technologie, Institut für Festkörperphysik, 76021 Karlsruhe, Germany

[1] Akira Iyo, Kenji Kawashima, Tatsuya Kinjo, Taichiro Nishio, Shigeyuki Ishida, Hiroshi Fujihisa, Yoshito Gotoh, Kunihiro Kihou, Hiroshi Eisaki, and Yoshiyuki Yoshida, "New-Structure-Type Fe-Based Superconductors: $CaAFe_4As_4$ (A = K, Rb, Cs) and $SrAFe_4As_4$ (A = Rb, Cs)," J. Am. Chem. Soc. **138**, 3410–3415 (2016).

[2] W. R. Meier, T. Kong, U. S. Kaluarachchi, V. Taufour, N. H. Jo, G. Drachuck, A. E. Böhmer, S. M. Saunders, A. Sapkota, A. Kreyssig, M. A. Tanatar, R. Prozorov, A. I. Goldman, Fedor F. Balakirev, Alex Gurevich, S. L. Bud'ko, and P. C. Canfield, "Anisotropic thermodynamic and transport properties of single-crystalline $CaKFe_4As_4$," Phys. Rev. B **94**, 064501 (2016).

[3] Daixiang Mou, Tai Kong, William R. Meier, Felix Lochner, Lin-Lin Wang, Qisheng Lin, Yun Wu, S. L. Bud'ko, Ilya Eremin, D. D. Johnson, P. C. Canfield, and Adam Kaminski, "Enhancement of the Superconducting Gap by Nesting in $CaKFe_4As_4$: A New High Temperature Superconductor," Phys. Rev. Lett. **117**, 277001 (2016).

[4] P. K. Biswas, A. Iyo, Y. Yoshida, H. Eisaki, K. Kawashima, and A. D. Hillier, "Signature of multigap nodeless superconductivity in $CaKFe_4As_4$," Phys. Rev. B **95**, 140505 (2017).

[5] Run Yang, Yaomin Dai, Bing Xu, Wei Zhang, Ziyang Qiu, Qiangtao Sui, Christopher C. Homes, and Xianggang Qiu, "Anomalous phonon behavior in superconducting $CaKFe_4As_4$: An optical study," Phys. Rev. B **95**, 064506 (2017).

[6] I. I. Mazin, D. J. Singh, M. D. Johannes, and M. H. Du, "Unconventional Superconductivity with a Sign Reversal in the Order Parameter of $LaFeAsO_{1-x}F_x$," Phys. Rev. Lett. **101**, 057003 (2008).

[7] Peter J. Hirschfeld, "Using gap symmetry and structure to reveal the pairing mechanism in fe-based superconductors," C. R. Physique **17**, 197 – 231 (2016), iron-based superconductors / Supraconducteurs base de fer.

[8] F. Kretzschmar, B. Muschler, T. Böhm, A. Baum, R. Hackl, Hai-Hu Wen, V. Tsurkan, J. Deisenhofer, and A. Loidl, "Raman-Scattering Detection of Nearly Degenerate s-Wave and d-Wave Pairing Channels in Iron-Based $Ba_{0.6}K_{0.4}Fe_2As_2$ and $Rb_{0.8}Fe_{1.6}As_2$ Superconductors," Phys. Rev. Lett. **110**, 187002 (2013).

[9] T. Böhm, A. F. Kemper, B. Moritz, F. Kretzschmar, B. Muschler, H.-M. Eiter, R. Hackl, T. P. Devereaux, D. J. Scalapino, and Hai-Hu Wen, "Balancing act: Evidence for a strong subdominant d-wave pairing channel in $Ba_{0.6}K_{0.4}Fe_2As_2$," Phys. Rev. X **4**, 041046 (2014).

[10] T. Böhm, F. Kretzschmar, A. Baum, M. Rehm, D. Jost, R. Hosseinian Ahangharnejhad, R. Thomale, C. Platt, T. A. Maier, W. Hanke, B. Moritz, T. P. Devereaux, D. J. Scalapino, S. Maiti, P. J. Hirschfeld, P. Adelmann, T. Wolf, H.-H. Wen, and R. Hackl, "Microscopic pairing fingerprint of the iron-based superconductor $Ba_{1-x}K_xFe_2As_2$," ArXiv e-prints (2017), arXiv:1703.07749 [cond-mat.supr-con].

[11] A. Bardasis and J. R. Schrieffer, "Excitons and Plasmons in Superconductors," Phys. Rev. **121**, 1050–1062 (1961).

[12] H. Monien and A. Zawadowski, "Theory of Raman scattering with final-state interaction in high-T_c BCS superconductors: Collective modes," Phys. Rev. B **41**, 8798–8810 (1990).

[13] D. J. Scalapino and T. P. Devereaux, "Collective d-wave exciton modes in the calculated Raman spectrum of Fe-based superconductors," Phys. Rev. B **80**, 140512 (2009).

[14] For details see Supplemental Material.

[15] W. R. Meier, T. Kong, S. L. Bud'ko, and P. C. Canfield, "Optimization of the crystal growth of the superconductor $CaKFe_4As_4$ from solution in the $FeAs{-}CaFe_2As_2{-}KFe_2As_2$ system," Phys. Rev. Materials **1**, 013401 (2017).

[16] Marianne Rotter, Marcus Tegel, and Dirk Johrendt, "Superconductivity at 38 K in the Iron Arsenide $(Ba_{1-x}K_x)Fe_2As_2$," Phys. Rev. Lett. **101**, 107006 (2008).

[17] J.-R. Scholz, *Raman Scattering Study of the Superconducting Pairing in* $CaKFe_4As_4$, Master's thesis, Technische Universität München (2017).

[18] W.-L. Zhang, W. R. Meier, T. Kong, P. C. Canfield, and G. Blumberg, "High T_c superconductivity in $CaKFe_4As_4$ in absence of nematic fluctuations," ArXiv e-prints (2018), arXiv:1804.06963 [cond-mat.supr-con].

[19] T. Cea and L. Benfatto, "Signature of the Leggett mode in the A_{1g} Raman response: From MgB_2 to iron-based superconductors," Phys. Rev. B **94**, 064512 (2016).

[20] Thomas P. Devereaux and Rudi Hackl, "Inelastic light scattering from correlated electrons," Rev. Mod. Phys. **79**, 175 (2007).

[21] Y. Gallais, R. M. Fernandes, I. Paul, L. Chauvière, Y.-X. Yang, M.-A. Méasson, M. Cazayous, A. Sacuto, D. Colson, and A. Forget, "Observation of Incipient Charge Nematicity in $Ba(Fe_{1-x}Co_x)_2As_2$," Phys. Rev. Lett. **111**, 267001 (2013).

[22] F. Kretzschmar, T. Böhm, U. Karahasanović, B. Muschler, A. Baum, D. Jost, J. Schmalian, S. Caprara, M. Grilli, C. Di Castro, J. H. Analytis, J.-H. Chu, I. R. Fisher, and R. Hackl, "Critical spin fluctuations and the origin of nematic order in $Ba(Fe_{1-x}Co_x)_2As_2$," Nature Phys. **12**, 560–563 (2016).

[23] V. K. Thorsmølle, M. Khodas, Z. P. Yin, Chenglin Zhang, S. V. Carr, Pengcheng Dai, and G. Blumberg, "Critical quadrupole fluctuations and collective modes in iron pnictide superconductors," Phys. Rev. B **93**, 054515 (2016).

[24] Pierre Massat, Donato Farina, Indranil Paul, Sandra Karlsson, Pierre Strobel, Pierre Toulemonde, Marie-Aude Méasson, Maximilien Cazayous, Alain Sacuto, Shigeru Kasahara, Takasada Shibauchi, Yuji Matsuda, and Yann Gallais, "Charge-induced nematicity in FeSe," Proc. Nat. Acad. Sciences **113**, 9177–9181 (2016).

[25] A. Baum, H. N. Ruiz, N. Lazarević, Y. Wang, T. Böhm, R. Hosseinian Ahangharnejhad, P. Adelmann, T. Wolf, Z. V. Popović, B. Moritz, T. P. Devereaux, and R. Hackl, "Frustrated spin order and stripe fluctuations in FeSe," ArXiv e-prints (2017), arXiv:1709.08998 [cond-mat.str-el].